Miner Deposita (2006) 41: 469–481
DOI 10.1007/s00126-006-0067-5

ARTICLE

Gi Young Jeong

Mineralogy and geochemistry of metalliferous black slates in the okcheon metamorphic belt, Korea: a metamorphic analogue of black shales in the South China block

Received: 4 April 2005 / Accepted: 31 March 2006 / Published online: 24 May 2006

Abstract Metalliferous black slates, which were locally exploited for their low-quality coal, are distributed in the Late Proterozoic to Paleozoic Okcheon Metamorphic Belt (OMB) of the Korean Peninsula. The mineralogy of the fine matrix is dominated by either quartz–(Ba, V)–mica–graphite or Quartz-Ba-feldspar–graphite. Polycrystalline submillimeter ellipsoids and elongate lenses aligned along foliations and veinlets are scattered through the fine matrix. Both ellipsoids and veinlets include many minor minerals containing rare elements: titanite, apatite, allanite, rutile, polycrase, barite, uraninite, xenotime, armenite, zircon, molybdenite, and sphalerite. Large graphite–apatite ellipsoids (nodules) with widths of several centimeters also occur in the highly carbonaceous black slates. Goldmanite occurs locally as porphyroblasts. The maximum rare element contents are: Ba 9.7%, V 2.04%, Mo 0.13%, U 0.11%, Cr 0.33%, Cu 254 ppm, Ni 479 ppm, Zn 607 ppm, Y 255 ppm, platinum-group element (PGE) + Au 309 ppb, and carbon 57%. The occurrence of the black slates and their elemental abundances suggests that most of the rare elements were accumulated from seawater in an oxygen-poor environment. However, the high Ba content of the OMB black slates indicates some hydrothermal input into an organic-rich basin. Although metamorphism and multiple deformations prevent a direct temporal and spatial correlation, metal abundances and a close association with graphite–apatite nodules and low-quality coal suggest that the OMB black slates are metamorphosed analogues of the Early Cambrian Ba–V deposits hosted by the black shales in the South China Block.

Keywords Black shale · Korea · Uranium · Vanadium · Barite

Editorial handling: R. Coveney Jr

G. Y. Jeong (✉)
Department of Earth and Environmental Sciences,
Andong National University,
Andong, 760-749, South Korea
e-mail: jearth@andong.ac.kr
Tel.: +82-54-8205619
Fax: +82-54-8231627

Introduction

Carbonaceous black slates in the Okcheon (also known as Ogcheon or Okchon) Metamorphic Belt (OMB) of South Korea, are thin beds that are rich in rare elements such as Ba, V, Mo, and U. They have been explored for their uranium since the discovery of radioactivity in the area in 1958; there has not been any metal mining (Kim 1989; Lee et al. 1986). The geology of the OMB has long been debated in regard to its tectonic setting, deposition, and metamorphic ages (Chang 2004; Cheong et al. 2003; Cho and Kim 2002; Chough et al. 2000; Cluzel et al. 1990; Lee et al. 1972, 1989; Min and Cho 1998; Ree et al. 1996, 2001; Yin and Nie 1993). The OMB is a key geological feature in the Korean Peninsula and therefore requires intensive investigation. The carbonaceous black slates, as unusual metasedimentary rocks occurring extensively throughout the Belt, may provide clues for the origin of the OMB. Geochemical studies carried out during uranium exploration found a high correlation between the uranium, vanadium, and molybdenum contents in the low-grade coal formation (Kim 1989; Lee and Chon 1980; Lee et al. 1986, 1996). Some mineralogical studies have been carried out on the black slates (Lee 1986; So and Kang 1978), but no detailed examination of the occurrence of rare metal-bearing minerals in the very fine carbonaceous matrix has been done. The depositional environment and the tectonic setting of the metalliferous black slates of the OMB have not been compared with those of other areas in East Asia. In this paper, the mineralogy and geochemistry of the black

slates analyzed in my laboratory are presented and discussed in relation to the Lower Cambrian metalliferous black shales occurring in the South China Block.

Geology of the OMB black slates

The most recent review of the geology of the OMB was carried out by Chough et al. (2000). The OMB is a NE-trending fold-and-thrust belt, bounded by the Precambrian Kyonggi Massif to the northwest, the Precambrian Yongnam Massif to the southeast, and the late Paleozoic sedimentary basin of Taebaeksan Zone to the northeast (Fig. 1). The Okcheon Supergroup consists of fossil-poor metasedimentary rocks (black slate, phyllite, schist, quartzite, conglomeratic phyllite, and dolomitic marble) and metavolcanic rocks (metarhyolite and amphibolite), which underwent low- to medium-grade metamorphism and were intruded by Jurassic and Cretaceous granitoids (Kim and Cho 1999; Min and Cho 1998; Oh et al. 1995).

Because the primary structures are mostly obliterated by metamorphism and polyphase deformation, the stratigraphic relationships between the formations are uncertain (Kang and Lee 2003; Koh and Kim 1995). The geologic age of the Okcheon Supergroup is not definitive, owing to a scarcity of fossils. Lee et al. (1998) reported a Late Proterozoic U–Pb age of 755.8±1.3 Ma from igneous zircons that were separated from metavolcanic rocks in the Munjuri Formation. A sample of Archaeocyatha from the dolomitic marble of the Hyangsanri Formation indicates a Cambrian age (Lee et al. 1972). Some conodonts and trilobites from a limestone pebble in the Hwanggangri Formation indicate an early Ordovician age (Lee et al. 1989). Isotopic dating of the peak metamorphism suffers from the presence of excess Ar, or from the low blocking temperatures of the K–Ar and Rb–Sr mica systems. The most reliable metamorphic ages are the Pb–Pb whole-rock isotopic ages of the black slates (Cheong et al. 2003), the U–Pb step-leaching ages of the metamorphic garnet from the garnet–amphibole schist (Kim et al. 2001), and the

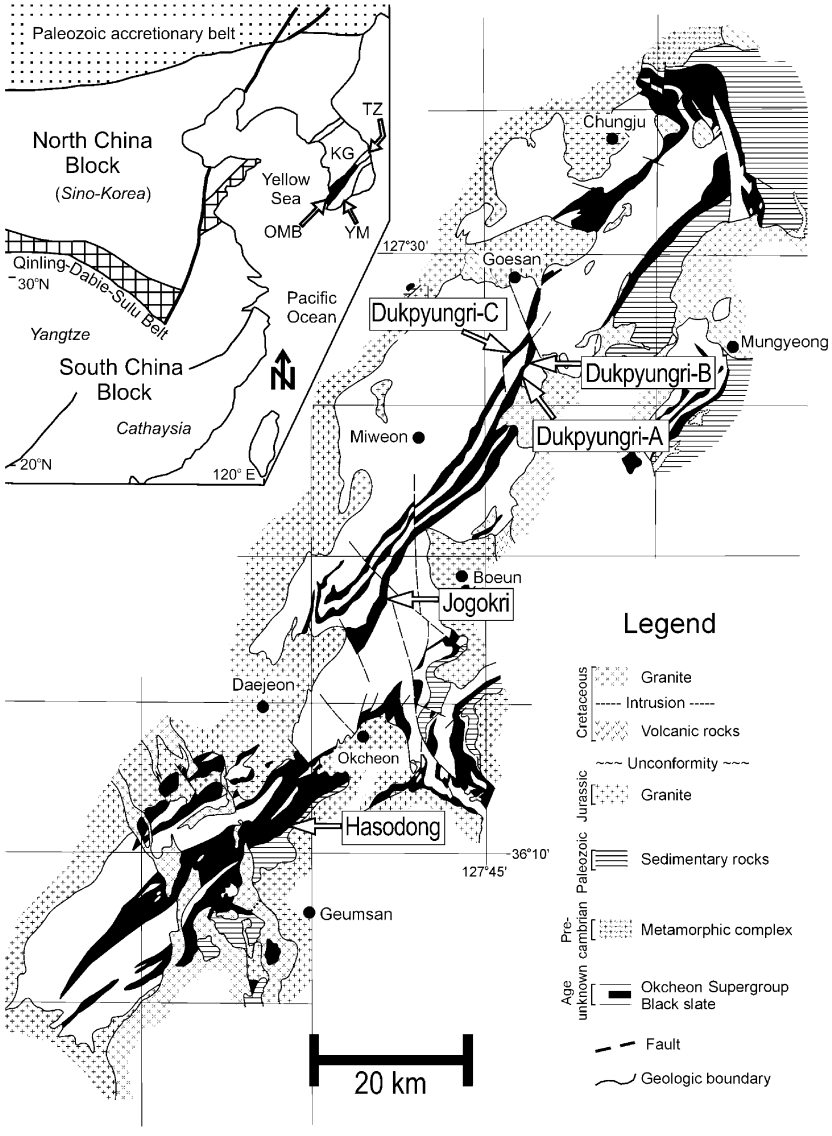

Fig. 1 Distribution of black slates in the Okcheon Metamorphic Belt (OMB) and locations of outcrops investigated in this study with tectonic map of northeast Asia (modified from Cheong et al. 2003). Age of the Okcheon Supergroup is not known but isotopic dating of metavolcanic rocks and several microfossils suggest Late Proterozoic to Early Paleozoic. *KG* Kyonggi Massif, *TZ* Taebaeksan Zone, *YM* Yongnam Massif

chemical Th–U–total Pb isochron method (CHIME) uraninite age of the black slates. These all indicate Early Permian peak metamorphism (280–290 Ma; Cheong et al. 2003). Therefore, the Okcheon Supergroup is composed of Late Proterozoic to possibly Early Paleozoic rocks, which experienced peak metamorphism in the Early Permian period.

The black slate is a collective term that includes carbonaceous black metasedimentary rocks. Although they are widespread in the OMB as shown in Fig. 1, metalliferous black slates with high carbon content form a very thin layer of about 20–40 m thick. Complex deformation and metamorphism make it difficult to recognize even the stratigraphically upper part of the black slate layers in the outcrops. The metalliferous black slates extend over 100 km in the OMB. Small-scale, low-grade coal mines operated locally to mine the highly carbonaceous parts of the metalliferous black slates.

The metalliferous black slates show well-developed cleavages but are locally massive in the highly carbonaceous parts. Veinlets of quartz and green mica commonly fill cracks in the black slates, forming complex patterns. In the weathered zone, secondary uranium minerals occur in radial crystals or as greenish-yellow to yellow colloidal precipitates.

Materials and methods

Metalliferous black slate samples for mineralogical and geochemical analyses were collected from the sites shown in Fig. 1: Dukpyungri-A, Dukpyungri-B, and Dukpyungri-C in Goesan; Jogokri in Boeun; and Hasodong in Daejeon. Outcrops exposing fresh black slate are rare because of the physical disintegration of the surface, but can be found locally at the abandoned small pits for low-grade coal mining or at recent road cuttings. The outcrops used for sampling were traced using a portable radioactivity detector. A series of hand-sized samples of different radioactivity and appearance was collected from the Dukpyungri-A outcrop across a bed of black slate that was ca. 50 m thick (Fig. 2). The sampling interval was narrowed in the highly radioactive part. Elemental analysis of the whole-rock samples was carried out using inductively coupled plasma emission spectroscopy for major elements and inductively coupled plasma mass spectroscopy for trace elements in the Activation Laboratories at Ancaster, Canada. Samples were decomposed by lithium metaborate/tetraborate fusion for major and trace element analyses. The platinum group element and Au contents were determined using neutron activation analysis of Activation Laboratories. The carbon content was determined using an elemental analyzer located at the Korea Basic Science Institute, Seoul. The major minerals in the black slates were identified using a Rigaku D/max 2000 X-ray diffractometer on whole-rock samples and, in some cases, on mineral separates. Trace minerals bearing rare metals were identified from polished thin sections using a JEOL JSM 6300 scanning electron microscope equipped with an energy-dispersive X-ray spectrometer. The mineral chemistry was determined using a Cameca SX50 electron microprobe analyzer. The detailed petrography was determined using a thin section of the black slates employing backscattered electron imaging combined with X-ray mapping.

Geochemistry

The major elemental compositions of the black slates are shown in Table 1. In the Dukpyungri-A outcrop, the carbon content increases towards the narrow part of the bed, up to a carbon content of 57 wt%. The maximum carbon content in the other outcrops ranges from 23 wt% (Dukpyungri-C) to 41 wt% (Hasodong). Barium is abundant in all samples (~9.7 wt%) and can be roughly correlated with the carbon content (Fig. 3a). Other metals enriched in the black slates are V (~2.0 wt%), Mo (~1,320 ppm), U (~1,090 ppm), Cr (~3,250 ppm), Zn (~607 ppm), Ni (~479 ppm), Cu (~254 ppm), and Y (~255 ppm) (Table 2). Vanadium is highly enriched in the carbonaceous black slate, but its content does not correlate with the carbon content (Fig. 3b). The vanadium content is relatively low in the samples of highly carbonaceous black slate from both the Dukpyungri-A and Hasodong outcrops, compared with other samples with relatively low carbon contents (Table 2). These two outcrops are different from other outcrops in their major mineral compositions: the former is rich in Ba-feldspar, whereas the latter is rich in (Ba, V)-muscovite. The U and Mo contents correlate positively with the carbon contents (Fig. 3c,d). The rare-earth element contents are high in the highly carbonaceous black slates (Fig. 3e). The total platinum-group element (PGE) plus Au contents are 59 ppb on average (Table 3, Fig. 3f). The PGE + Au contents vary significantly between samples with a maximum content of 309 ppb at the Dukpyungri-B outcrop. The Ir/Pd ratios range from 0.0045 to 0.24.

Microfabrics and mineralogy

Matrix

Graphite and quartz are the major matrix minerals common to all samples and are consistently associated with Ba–

Fig. 2 Photograph of the outcrop of metalliferous black slate at the Dukpyungri-A site with sample positions. There is a gap about 10 m wide due to stream incision

Table 1 Major element contents of black slates

Sample	SiO_2	Al_2O_3	Fe_2O_3	MnO	MgO	CaO	Na_2O	K_2O	TiO_2	P_2O_5	BaO	LOI	Total	C
Dukpyungri (A)														
1	–	4.15	1.96	0.006	0.07	0.16	0.03	1.04	0.290	0.07	0.63	–	–	4.3
5	–	3.35	0.38	0.006	0.38	0.66	0.07	1.60	0.230	0.22	7.37	–	–	42.7
6	32.59	8.62	0.37	0.011	0.70	1.29	0.15	1.99	0.460	0.54	10.05	42.05	98.82	38.0
7	31.47	8.84	2.69	0.026	1.68	3.19	0.13	1.76	0.354	0.71	8.42	40.45	99.72	40.0
9	–	4.11	1.72	0.014	0.77	1.69	0.07	1.55	0.160	0.26	5.47	–	–	36.9
12	40.66	6.36	2.21	0.018	0.76	1.51	0.17	1.50	0.250	0.24	5.75	38.65	98.08	38.8
16	48.90	3.27	0.53	0.020	2.14	2.03	0.14	0.61	0.230	0.50	4.06	35.92	98.35	34.5
20	–	5.26	1.54	0.015	1.02	2.18	0.10	1.62	0.260	0.36	7.59	–	–	31.5
22	39.41	10.11	2.52	0.022	1.57	2.44	0.19	2.10	0.388	0.66	10.83	28.79	99.03	26.2
25	26.25	4.99	0.48	0.004	0.32	0.62	0.10	0.90	0.288	0.25	7.30	58.29	99.76	57.1
27	54.22	3.41	6.28	0.086	6.57	8.31	0.10	0.36	0.180	0.21	3.96	16.35	100.03	14.1
29	–	5.64	0.59	0.013	0.78	1.57	0.13	2.94	0.460	0.10	6.48	–	–	8.9
30	60.45	9.40	2.34	0.106	2.76	7.04	0.27	2.21	0.526	0.43	1.93	12.55	100.02	9.9
32	69.02	8.48	0.81	0.054	1.29	2.89	0.14	2.37	0.462	0.58	1.30	13.03	100.43	9.4
34	65.72	11.01	0.82	0.053	0.95	2.61	0.12	3.07	0.613	0.88	1.33	13.22	100.40	8.5
Dukpyungri (B)														
GS9701	60.03	5.83	1.52	0.014	1.25	0.33	0.12	1.34	0.315	0.40	2.84	22.80	96.79	20.3
GS9702-1	29.78	10.88	5.58	0.030	2.99	0.26	0.24	2.46	0.979	0.43	7.02	37.70	98.35	31.2
Dukpyungri (C)														
DJA	56.03	14.29	0.61	0.004	1.22	0.03	0.28	4.20	0.635	0.05	3.54	14.65	95.54	14.0
DJB	52.06	14.62	0.55	0.004	1.12	0.36	0.25	3.74	0.903	0.42	3.91	20.67	98.61	19.5
DJC	52.95	13.46	5.72	0.005	1.10	0.02	0.25	3.69	0.613	0.12	3.25	15.23	96.41	13.4
DJ1	56.61	8.35	6.38	0.011	0.67	0.81	0.12	2.07	0.343	0.48	1.86	19.84	97.54	15.6
DJ42	49.32	8.67	2.14	0.010	1.57	1.59	0.08	2.73	0.337	1.24	2.19	26.90	96.78	23.4
Jogokri														
JG-A	41.67	18.29	1.92	0.003	1.11	0.02	0.13	5.29	0.798	0.10	3.29	23.51	96.13	20.3
JG-B	61.43	20.89	1.40	0.005	1.00	ND	0.28	6.25	0.714	0.03	0.74	5.11	97.84	2.1
JG4C	44.49	18.01	2.57	0.004	1.13	0.03	0.20	5.39	0.926	0.12	3.45	20.25	96.57	17.1
JG6A	36.12	7.88	2.73	0.053	1.69	3.30	0.11	2.37	0.479	0.91	2.14	39.74	97.52	35.6
JG6B	42.78	3.81	3.49	0.083	2.40	5.34	0.01	1.09	0.218	0.60	1.29	37.88	98.99	32.0
JG7	27.14	7.28	4.19	0.146	4.73	9.31	0.07	2.28	0.420	0.76	3.34	38.97	98.64	29.0
JG8	40.91	6.61	5.37	0.074	2.26	5.09	0.08	1.84	0.249	0.74	1.43	34.27	98.92	27.9
JG9	73.82	2.56	4.02	0.053	1.74	3.46	Nd	0.58	0.084	0.30	0.53	12.30	99.44	8.6
JG10	48.65	4.65	4.44	0.106	3.17	6.05	0.20	1.52	0.176	0.41	2.07	25.24	96.69	17.6
Hasodong														
CB600	52.16	8.87	4.49	0.068	3.01	5.64	0.23	3.26	0.549	0.16	6.35	12.07	96.86	9.8
CB1200	30.94	9.24	1.33	0.006	0.40	1.33	0.18	3.54	0.637	0.72	5.85	43.27	97.44	41.0
CB1400	40.21	11.58	2.16	0.062	1.26	4.29	0.44	4.01	0.756	1.16	3.18	28.67	97.78	25.1
CB3000	33.89	12.18	2.96	0.017	0.47	3.52	0.09	0.09	0.408	0.72	5.41	38.56	98.32	31.4

Values are in wt%. SiO_2 and loss on ignition (LOI) of some samples were not determined. *Nd* Not detected

aluminosilicates. The Tagiri graphitizing-degree ranges from 31 to 100, corresponding to temperatures of 350 to 550 °C under a maximum load pressure of 5.5 kbar (Na et al. 1988). In general, Ba–aluminosilicate closely associated with quartz and graphite in the matrix is either (Ba, V)-rich green muscovite in the Dukpyungri-B (Fig. 4a,b), Dukpyungri-C, and Jogokri (Fig. 4c,d) or hyalophane in the Dukpyungri-A (Fig. 5a–c) and Hasodong samples. The (Ba, V)-rich muscovite contains ca. 1.9 wt% BaO and 2.8 wt% V_2O_3 but cannot be classified as a (Ba, V)-analogue of muscovite because the number of Ba and V per $O_{20}(OH)_4$ does not exceed half the number of sites. The mole percent of celsian in hyalophane is in the range of 19.9 to 80.1%. The lower V contents in the highly carbonaceous black slates of the Dukpyungri-A and Hasodong samples compared with the V contents of the Dukpyungri-B, Dukpyungri-C, and Jogokri areas are consistent with the fact that hyalophane is the major barian mineral in the former black slates.

Uraninite (Fig. 5d), zircon (Fig. 4a), apatite (Fig. 4a), xenotime, and molybdenite (Fig. 5b) are occasionally scattered in the matrix. In particular, barite is more common in the Dukpyungri-A samples and closely associated with high-Ba hyalophane. The textural relation-

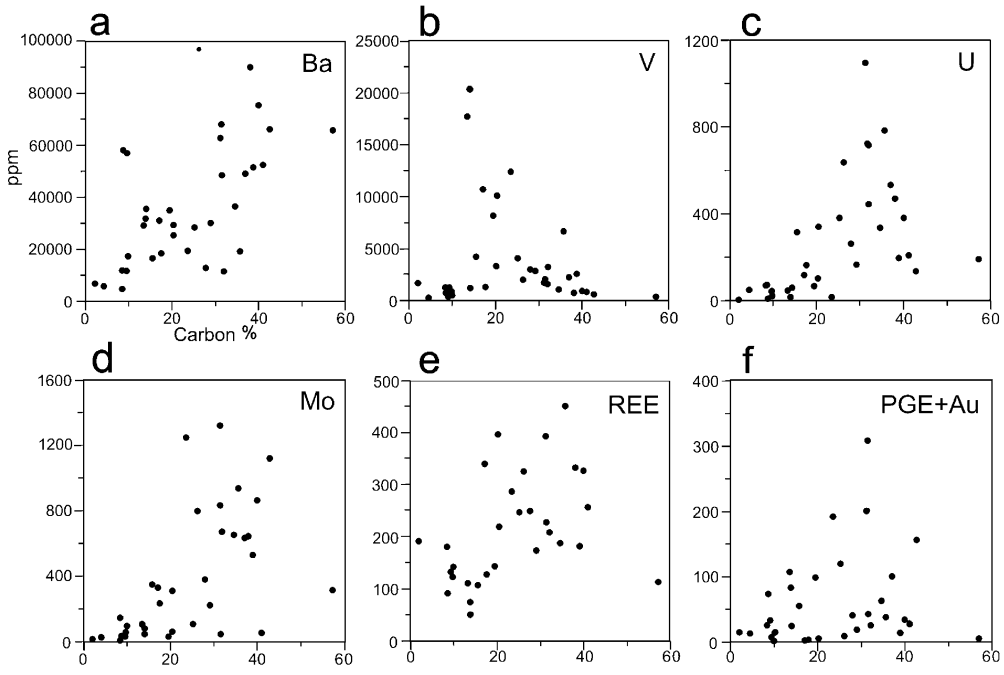

Fig. 3 Plot of metal contents vs carbon content in the OMB black slates

ship (see inset in Fig. 5a) suggests that hyalophane replaced barite from the grain edge inwards.

Polycrystalline aggregates

Submillimeter-size polycrystalline aggregates occur in the form of ellipsoids and elongated lenses that are aligned along metamorphic foliation or veinlets occurring throughout the opaque carbonaceous matrix. The most abundant are the well-formed ellipsoids of polycrystalline quartz (Fig. 6a) that are occasionally associated with apatite (Fig. 6a,b), (Ba, V)-muscovite (Fig. 6c), and uraninite (Fig. 6c–e). Titanite includes tiny grains of uraninite and barite (Fig. 6e). Jeong and Lee (2001) reported pyrite, sphalerite, molybdenite, and rutile inclusions in titanite. Macroscopic nodular ellipsoids of graphite–apatite that are several centimeters in diameter have been reported as being scattered in the highly carbonaceous layers of the black slates (Shim et al. 1995). Foliation enclosing these graphite–apatite ellipsoids indicates that they were formed before metamorphism (Fig. 7a). Figure 7b shows the interior details of the graphite–apatite ellipsoids. The polycrystalline elongate lenses include hyalophane–barite (Fig. 8a,b), barite–rutile–quartz–hyalophane–celsian (Fig. 8c,d), quartz–apatite–barite (Fig. 8e,f), allanite, and rutile–polycrase–quartz. Uraninite cubes, which are several micrometers in diameter, were often included in the quartz-rich ellipsoids and polycrystalline elongate lenses. Figure 8b shows a formation sequence of Ba-bearing minerals from barite to a low-Ba hyalophane via a high-Ba hyalophane.

Although uraninite grains are occasionally scattered in the matrix (Fig. 5d), most of the uraninite crystals suitable for dating by CHIME employing electron microprobe analysis were found within the polycrystalline aggregates of the ellipsoids and elongate lenses (Figs. 6c–e and 8b,f). Cheong et al. (2003) reported CHIME ages of uraninite as 283±26 Ma in the Dukpyungri-A area and 281±27 Ma in the Jogokri area. These data are consistent (within the given error ranges) with the $^{207}Pb/^{206}Pb$ ages of the Dukpyungri-A and Jogokri areas of 283±33 and 291±13 Ma, respectively (Cheong et al. 2003).

Microfissures

Microfissures cutting the fine-grained matrix are filled with noncarbonaceous minerals of rare elements. The veinlets were repeatedly cut or folded in a complex pattern involving several stages of deformation. The mineral species of the veinlets are not different from those of the matrix and polycrystalline ellipsoidal and elongate lenses. The veinlets in the hyalophane-rich black slates contain quartz and hyalophane (Fig. 9a), whereas those in the (Ba, V)-muscovite-rich black slates consist of (Ba, V)-muscovite and quartz with molybdenite (Fig. 9b). Other rare minerals in the veinlets are allanite (Fig. 9c), armenite (Fig. 9d), monazite (Fig. 9e), and dolomite (Fig. 9f). Although uraninite was not generally found in the quartz or quartz–muscovite veinlets, uraninite inclusions in calcite within dolomite veinlets of the Jogokri sample (Fig. 9f) gave a CHIME age of 261±15 Ma. This age is only slightly younger than the uraninite in the matrix, ellipsoidal, and elongate lenses.

Porphyroblasts

By the later stages of deformation/metamorphism, porphyroblasts grew in some parts of the black slate sequence. In the Dukpyungri-A area, goldmanite and diopside occur

Table 2 Trace element contents (parts per million) of black slates

Sample	V	Cr	Ni	Cu	Zn	Y	Mo	Ba	Pb	Th	U	REE_{total}	C(wt%)	S(wt%)
Dukpyungri (A)														
1	178	47	297	23	109	38	22	5,600	13	5.9	50	–	4.3	0.0
5	606	300	17	12	29	221	1,112	66,000	93	10.0	140	–	42.7	0.8
6	740	105	Nd	75	33	240	541	89,973	8	9.8	471	331.6	38.0	0.5
7	856	65	293	73	33	75	427	75,382	83	11.2	377	327.4	40.0	1.0
9	2,260	490	303	108	243	160	633	49,000	63	7.1	530	–	36.9	1.3
12	2,566	143	361	147	547	102	202	51,529	7	5.3	197	181.3	38.8	0.9
16	1,016	44	Nd	17	Nd	127	104	36,360	35	4.4	338	185.7	34.5	0.3
20	1,577	600	106	135	50	253	828	68,000	67	8.9	720	–	31.5	0.8
22	2,005	231	212	88	52	142	764	96,957	19	10.6	636	326.3	26.2	1.6
25	271	22	39	39	76	54	101	65,366	186	8.2	191	112.8	57.1	0.7
27	1,232	35	176	42	532	23	44	35,433	14	3.3	59.5	51.3	14.1	0.1
29	387	640	24	12	15	58	29	58,000	15	11.0	15	–	8.9	0.1
30	889	55	124	62	165	35	93	17,314	6	9.5	31.8	142.4	9.9	0.7
32	1,222	81	211	119	116	36	35	11,638	6	8.2	43.0	131.0	9.4	0.0
34	677	84	208	128	124	46	9	11,921	8	11.1	68.0	180.1	8.5	0.0
Dukpyungri (B)														
GS9701	3,247	109	47	31	Nd	98	63	25,410	68.9	8.3	338	220.0	20.3	–
GS9702-1	1,686	102	295	121	77	159	1,320	62,910	107	22.4	1,090	393.8	31.2	–
Dukpyungri (C)														
DJA	20,375	3,250	Nd	38	Nd	150	81	31,716	27	12.1	17.8	74.0	14.0	–
DJB	8,150	301	Nd	63	Nd	75	30	35,019	61	12.5	68.0	143.6	19.5	–
DJC	17,738	2,660	35	258	90	85	300	29,096	26	13.2	52.9	110.4	13.4	–
DJ1	4,239	102	213	151	296	94	348	16,660	57.6	8.0	317	106.5	15.6	–
DJ42	12,420	369	Nd	11	47	143	1,250	19,610	461	7.0	20.0	288.8	23.4	–
Jogokri														
JGA	10,100	608	Nd	91	Nd	255	313	29,470	56.0	25.6	102	396.2	20.3	–
JGB	1,645	211	21	Nd	Nd	60	9	6,672	3.81	8.3	2.8	190.9	2.1	–
JG4C	10,750	522	Nd	141	Nd	186	329	30,920	29.0	21.2	118	339.2	17.1	–
JG6A	6,677	124	763	100	51	374	933	19,140	73.9	14.4	782	450.2	35.6	–
JG6B	3,211	71	295	170	Nd	176	671	11,560	48.0	6.6	445	209.1	32.0	–
JG7	2,868	144	294	86	Nd	121	223	29,940	26.9	8.7	169	173.2	29.0	–
JG8	3,058	129	145	119	607	159	378	12,790	74.6	5.9	263	249.4	27.9	–
JG9	1,219	50	275	254	Nd	46	143	4,718	9.57	2.4	73.7	90.8	8.6	–
JG10	1,288	46	192	170	Nd	64	234	18,570	18.5	5.0	167	127.9	17.6	–
Hasodong														
CB600	560	31	118	17	120	31	54	56,890	4.43	12.0	27.3	121.4	9.8	–
CB1200	787	52	40	47	115	66	55	52,360	19.9	16.5	207	256.7	41.0	–
CB1400	4,094	113	479	254	196	148	109	28,460	68.3	22.0	380	245.6	25.1	–
CB1300	2,006	115	307	92	234	94	44	48,500	29.7	11.5	726	228.10	31.4	–

Rare earth elements (REE) and sulfur of some samples were not determined. *Nd* Not detected

as porphyroblasts, cutting foliations defined by hyalophane, quartz, and graphite. Goldmanite (~30 wt% V_2O_3), the green vanadium end-member of the garnet solid solution, has a radial growth habit, as reported by Jeong and Kim (1999); goldmanite commonly overgrew cores of uraninite and barite (Fig. 10). In contrast, diopside has a poikilitic texture with numerous inclusions of matrix minerals.

Discussion

Source of metals and environments

The OMB black slates underwent low- to medium-grade metamorphism, during which their chemical composition may have changed. However, the long lateral extent of the metalliferous black slates along the OMB and the enrichment of rare metals in narrow carbonaceous horizons of 20–40 m thickness indicate that metals were not significantly added or subtracted during metamorphism.

Table 3 Platinum group element (PGE) and Au analysis of black slates (in parts per billion)

Sample	Os	Ir	Ru	Rh	Pt	Pd	PGE	Ir/Pd	Au	PGE + Au	C(%)
Dukpyungri-A											
1	Nd	0.3	Nd	0.7	Nd	Nd	1		12	13	4.3
5	10	Nd	Nd	Nd	16	Nd	26		130	156	42.7
7	Nd	0.3	Nd	Nd	16	12	28	0.025	4.9	33	40.0
9	4	1	Nd	Nd	15	Nd	20		81	101	36.9
12	Nd	Nd	Nd	Nd	8	Nd	8		5.3	13	38.8
16	Nd	0.5	Nd	0.6	13	42	56	0.012	6.4	63	34.5
20	16	1.6	Nd	Nd	12	Nd	30		14	44	31.5
22	Nd	0.1	Nd	Nd	Nd	Nd	0		8.4	9	26.2
25	Nd	0.2	Nd	Nd	Nd	Nd	0		4.2	4	57.1
27	Nd	0.1	Nd	Nd	Nd	22	22	0.005	2.6	25	14.1
29	Nd	0.3	Nd	Nd	Nd	15	15	0.020	17	32	8.9
30	Nd	Nd	Nd	Nd	Nd	Nd	0		1.3	1	9.9
32	Nd	0.2	Nd	Nd	Nd	6	6	0.033	1.8	8	9.4
34	Nd	1.2	Nd	Nd	Nd	5	6	0.240	20	26	8.5
Dukpyungri-B											
GS9702-1	5	1.3	6	Nd	180	46	238	0.028	71	309	31.2
Dukpyungri-C											
DJA	Nd	0.5	Nd	1.2	55	Nd	57		26	83	14.0
DJB	Nd	Nd	Nd	0.4	33	47	80		18	98	19.5
DJC	4	0.5	Nd	4.5	51	39	99	0.013	8.9	108	13.4
DJI	4	1.8	Nd	1.1	Nd	Nd	7		48	55	15.6
DJ42	25	0.7	30	0.4	20	66	142	0.011	50	192	23.4
Jogokri											
JGA	Nd	0.2	Nd	0.5	Nd	Nd	1		4.9	6	20.3
JGB	Nd	0.3	Nd	Nd	Nd	Nd	0		14	14	2.1
JG4C	Nd	0.2	Nd	Nd	Nd	Nd	0		2	2	17.1
JG6A	Nd	0.6	Nd	3.7	Nd	Nd	4		34	38	35.6
JG6B	Nd	0.2	Nd	0.2	Nd	22	22	0.009	4	26	32.0
JG7	Nd	0.2	Nd	Nd	Nd	Nd	0		19	19	29.0
JG8	6	0.3	Nd	Nd	Nd	32	38	0.009	2.3	41	27.9
JG9	7	0.3	Nd	Nd	Nd	60	67	0.005	5.6	73	8.6
JG10	Nd	0.2	Nd	0.5	Nd	Nd	1		1.1	2	17.6
Hasodong											
CB600	Nd	0.3	Nd	Nd	7	−5	7		6.7	14	9.8
CB1200	3	0.3	Nd	0.4	Nd	23	27	0.013	3.2	30	41.0
CB1400	12	0.6	Nd	Nd	15	65	93	0.009	27	120	25.1
CB3000	10	1.9	Nd	Nd	167	−5	179		23	202	31.4

Nd Not detected

The average metal contents of the OMB black slates correlate overall with those of seawater, whereas the Mo and U contents of average crust (Mason and Moore 1982) and average shale (Turekian and Wedepohl 1961) are exceptionally low when compared with seawater (Li 1991) (Fig. 11a). Thus, it is suggested that the metals enriched in the OMB black slates originated from seawater. However, Ba, V, U, and Mo are much more concentrated than in the highly carbonaceous Alum Shale in Sweden (Leventhal 1991) and Mecca Quarry black shale in North America (Vine and Tourtelot 1970; Coveney and Martin 1983), whereas Cu, Zn, and Ni are less concentrated (Fig. 11b). Holland (1979) showed that metal enrichment in black shales was mostly attributable to precipitation from seawater; however, the exceptionally high enrichment of some elements relative to their concentration in seawater requires other processes to be at work. The high Ba content in the black slates may be attributable to Ba arising from hydrothermal venting into the oxygen-poor basin or organic-rich sediment.

One of the key features of the OMB black slates is a very low content of sulfides. Pyrite, generally a widespread mineral in organic sediments, is very rare in the OMB black slates. Their Cu, Zn, and Ni contents are lower than those

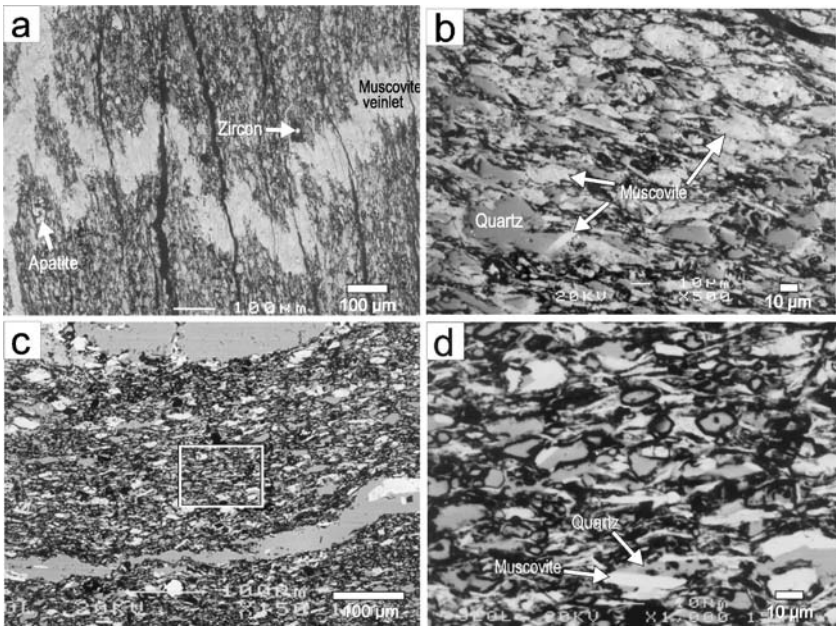

Fig. 4 Backscattered electron images of micaceous matrix of the black slate. Black is graphite. **a** Sample DJ42 from Dukpyungri-C. **b** Magnified image of **a**. **c** Sample J6A from Jogokri. **d** Image magnified from the box in **c**

found in other metalliferous black shales (Fig. 11b), which may be related to the relatively low levels of sulfide in the water column. Despite the high carbon content, the low sulfide level indicates that the submarine depositional environment was not anoxic but dysoxic (0.1 to 1.0 mg/l O_2) (Arthur and Sageman 1994).

Although barite is found as a minor mineral in the OMB black slates, it is more common in the Dukpyungri-A area. As shown in Figs. 5a and 8b, it appears that primary barite was replaced partly by high-Ba hyalophane. Although the major Ba minerals are Ba-feldspars and (Ba, V)-micas, barite was originally more abundant before metamorphism, given that barite has been replaced by high-Ba hyalophane. Because the seawater sulfate would have been only partially reduced to sulfide under dysoxic conditions, barite could precipitate from Ba-rich hydrothermal fluids venting into the basin. Barium could have been also adsorbed on the clay minerals, along with V or possibly amorphous biogenic silica in the organic-rich sediments (Kříbek et al. 1996). Low levels of reduced sulfur species would have limited the precipitation of Zn, Ni, and Cu sulfides. However, a low concentration of base metals in the venting hydrothermal fluid cannot be ruled out. The PGE elements that are relatively abundant in the highly carbonaceous OMB black slates were most likely introduced by submarine hydrothermal activity.

The carbon content of the OMB black slates is very high, up to 57 wt%. Although the carbon content may have been increased by the loss of volatiles during metamorphism and deformation, organic matter must have been a major

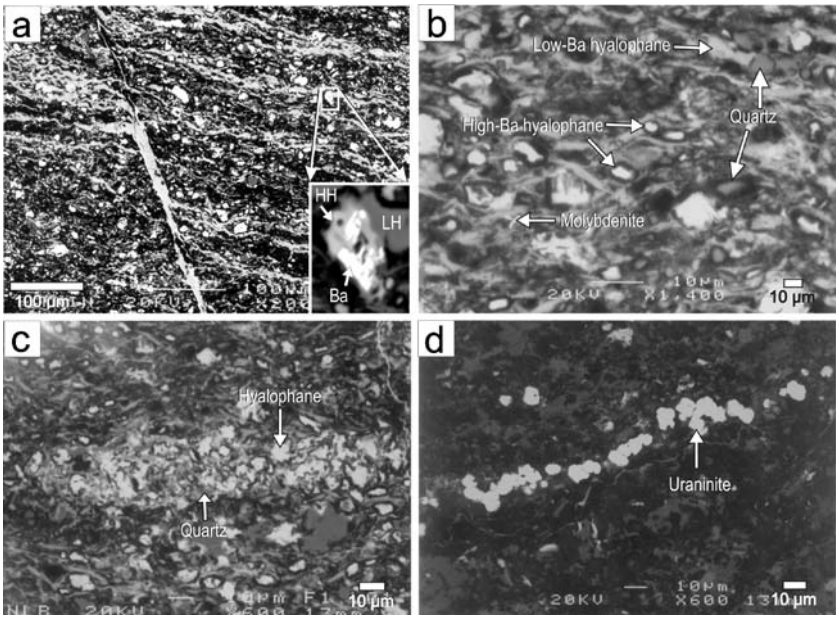

Fig. 5 Backscattered electron images of feldspathic matrix of the black slate. Black is graphite. **a** Sample 22 from Dukpyungri-A. *Inset* shows the replacement of barite (Ba) by high-Ba hyalophane (HH). *LH* Low-Ba hyalophane. **b**–**d** Magnified images of **a**

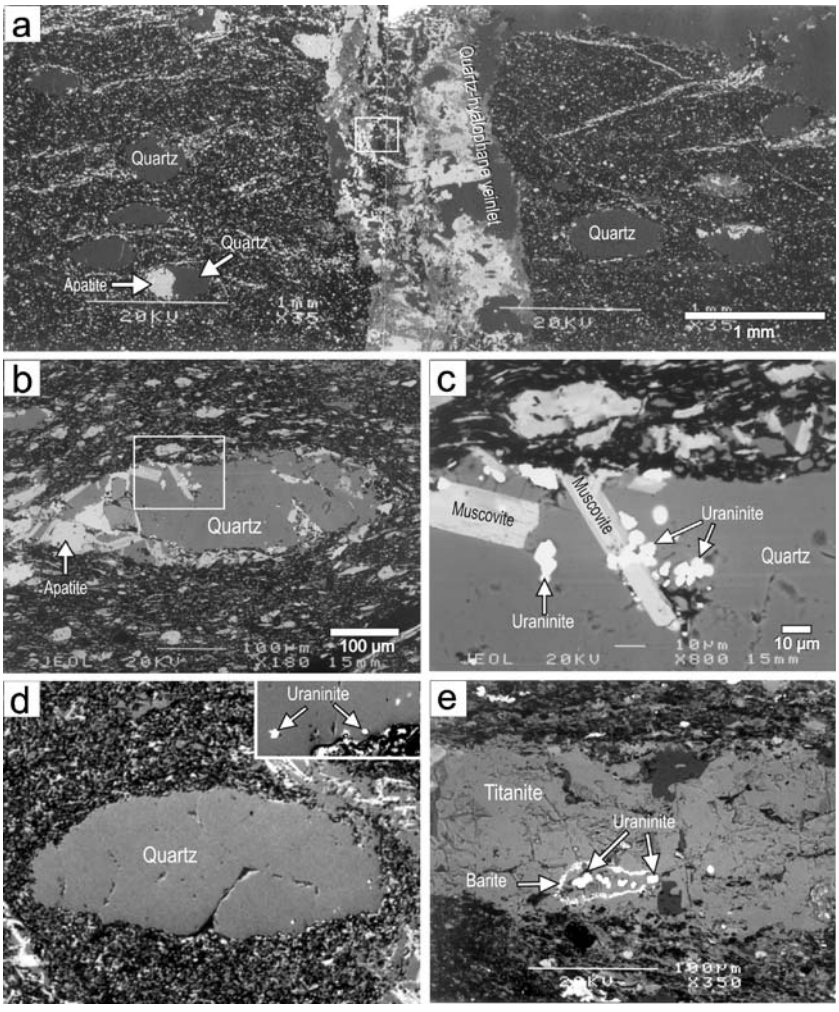

Fig. 6 Backscattered electron images of submillimeter ellipsoids in the black slates. Black is graphite. **a** Sample 9 from Dukpyungri-A. The box is magnified in Fig. 9a. **b** Sample J6A from Jogokri. **c** Magnified image of the box in **b**. **d** Sample DJ1 from Dukpyungri-C. **e** Sample 22 from Dukpyungri-A

component of the original sediment of the OMB black slates. A high carbon content is possible in deep, open basins, such as those in continental slopes undergoing coastal upwelling and high productivity, as found in the modern offshore sediments of Peru and Namibia (Arthur and Sageman 1994). However, submarine hydrothermal activity typically occurs along mid-ocean ridges and back-arc basins (Douville et al. 1999). Although the tectonic setting and paleogeography of the OMB are not certain, laterally extensive, thick, and highly organic sediments are not normally deposited in a mid-ocean ridge-type environment. Hydrocarbon formation via hydrothermal processes was reported in organic-rich sediments of the Guaymas Basin, Gulf of California, which is a part of the East Pacific Rise (Peter et al. 1990). But the depositional environment of high biological productivity and influx of terrigenous detritus in the Gulf of California is similar to back-arc basin environments. Therefore, I suggest that the organic-rich metalliferous sediments of the OMB were deposited in a narrow basin connected to the open sea, which had a submarine hydrothermal system related to rifting in a back-arc setting.

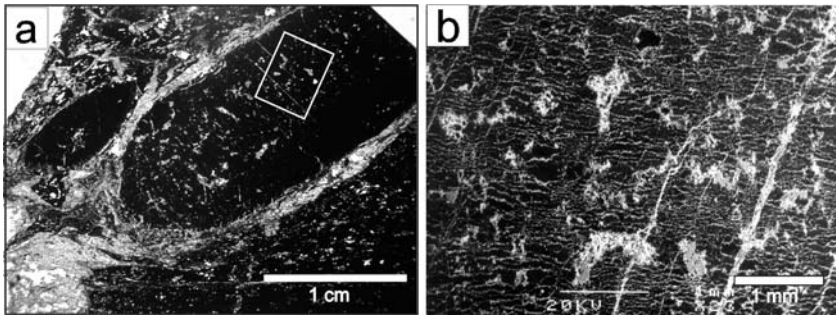

Fig. 7 **a** Photomicrograph of graphite–apatite ellipsoids in the highly carbonaceous black slate. *Black* is graphite. *Thinsection* Plane-polarized light. **b** Backscattered electron image of the box in **a**. *Gray* Apatite, *Black* graphite

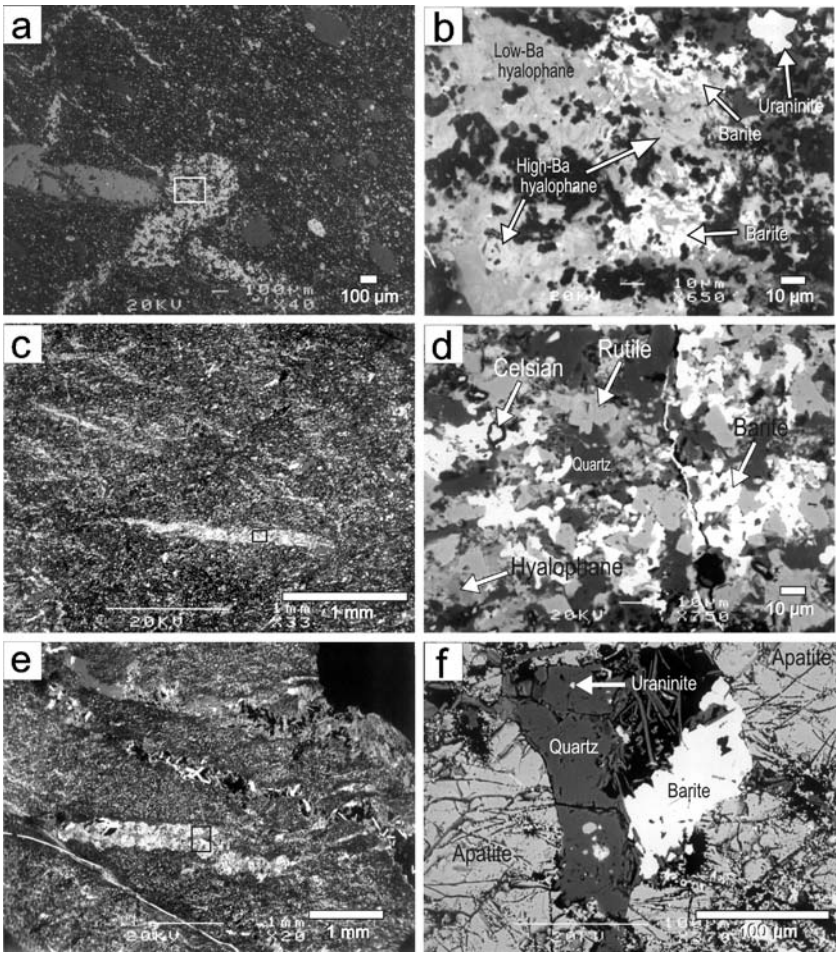

Fig. 8 Backscattered electron images of polycrystalline elongate lens. *Black* is graphite. **a** Sample 22 from Dukpyungri-A. **b** Image magnified from the box in **a**. **c** Sample GS9702 from Dukpyungri-B. **d** Image magnified from the box in **c**. **e** Sample GS9702 from Dukpyungri-B. **f** Image magnified from the box in **e**

Correlation with the black shales of the South China Block

Lower Cambrian black shales are widespread in the South China Block and include numerous syngenetic or sedimentary exhalative mineral deposits of Ni, Mo, V, Ba, U, P, and coal (Chen et al. 1990; Coveney and Chen 1991; Coveney et al. 1994; Fan 1983). Four distinct facies can be distinguished for the Late Sinian to Early Cambrian interval: a carbonate platform, a protected basin (former back-arc basin), the Jiangnan uplift (former arc), and a deep oceanic basin (Steiner et al. 2001). Fan (1983) classified the economic mineral deposits enclosed in the Lower Cambrian black shale series into phosphorites, stone coals, V–Ba deposits, and Ni–Mo deposits.

Chen et al. (1990) showed that the Ni–Mo deposits are distributed in areas belonging to the transitional belt and the Yangtze sedimentary basin, which correspond to a carbonate platform. The V–Ba deposits, meanwhile, are largely concentrated in the transitional belt and sedimentary basin south of the Yangtze River defined by the biogeography, which roughly corresponds to the protected basin of Steiner et al. (2001). Syngenetic Early Cambrian Ni–Mo–PGE–Au sulfide deposits (>2 wt% Mo, >2 wt% Ni) are hosted by the basal layer of the black shales of the Niutitang Formation that are linearly distributed along the Guizhou, Hunan, Jiangxi, and Zhejiang areas, and are mined locally for their high Ni and Mo contents (Coveney and Chen 1991). Sulfur isotopes, ore fabrics, fossil assemblages, and abnormal metal contents indicate a sedimentary exhalative origin in the shallow sedimentary basin near the continental margin (Lott et al. 1999; Murowchick et al. 1994; Steiner et al. 2001).

The vanadium ore beds associated with black shales in the South China Block consist of black silty shales, siliceous rocks, and phosphatic nodular shales having thicknesses between 10 and 20 m. Vanadium is mostly incorporated in vanadian illite and is uniform in content throughout the beds (1–2 wt% V_2O_3). The vanadium ore is closely associated with stone coal, a combustible low-quality sapropelic anthracite, made up of the remains of algae and fungi, which accounts for about 1% of the coal reserves in China (Chen et al. 1990; Coveney et al. 1994). The carbon content of this "stone coal" ranges from 10 to 20 wt% but can be as high as 40 to 50 wt% (Chen et al. 1990). The stone coal seams consist largely of black carbonaceous shales, siliceous rocks, and siltstone that are mostly distributed in the sedimentary basin south of the Yangtze River. A variety of metals such as Ni, Mo, V, Cu, U, Yb, Ag, and P are commonly associated with these deposits. Barium mostly occurs as authigenic barite, which

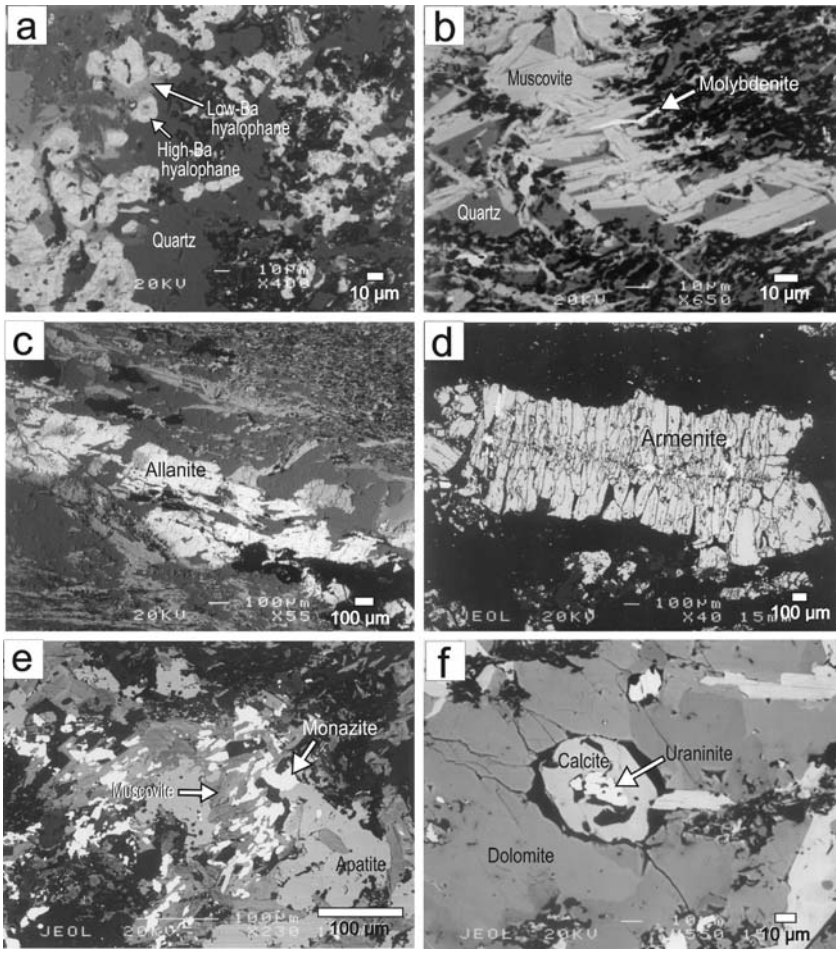

Fig. 9 Backscattered electron images of veinlets. *Black* is graphite. **a** Feldspathic veinlet. Image magnified from the box of the veinlet in Fig. 6a. **b** Micaceous veinlet. Sample DJ1 from Dukpyungri-C. **c** Allanite veinlet. Sample DJ42 from Dukpyungri-C. **d** Armenite veinlet. Sample CB3000 from Hasodong. **e** Monazite in veinlet. Sample J6A from Hasodong. **f** Uraninite in dolomite veinlet. Sample J6A from Jogokri

is widely distributed in the black shale, black chert, and phosphorite concretions (Fan 1983).

The metal content of the OMB metalliferous black slates is not as high as that of the Early Cambrian Ni–Mo sulfide deposits of the Chinese black shales, but the V and Mo contents are somewhat similar to those of the vanadium deposits (Fig. 11c). Sulfide is a minor component in the OMB black slates, and the carbon content is similar to that in the metamorphosed stone coal of the Chinese black shale series. The vanadian illite may have been recrystallized into (Ba, V)-muscovite during metamorphism. The graphite–apatite ellipsoids resemble the phosphatic nodules associated with the Ba-V deposits. Long et al. (1994) reported on hyalophane-rich carbonaceous black siliceous rocks occurring in the lower Cambrian black shale series located in the basin between the Jiangnan Island Arc and the Yangtze Plate. The hyalophane-rich OMB black slates may be the metamorphosed analogue of the hyalophane-

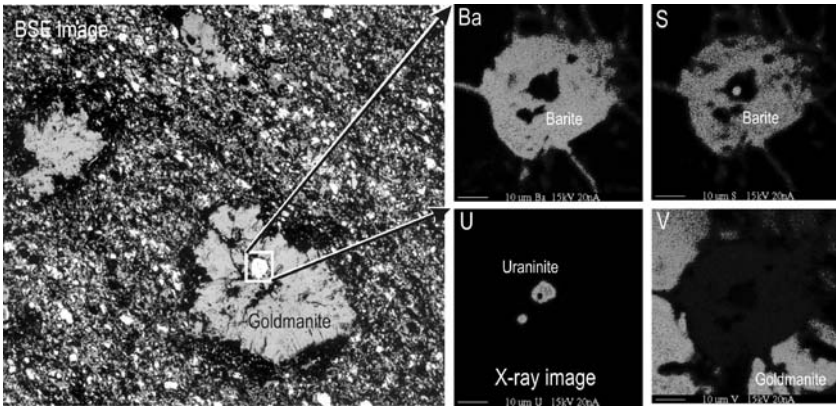

Fig. 10 Goldmanite overgrowth on uraninite–barite. Sample 22 from Dukpyungri-A. Backscattered electron image and wavelength dispersive X-ray elemental map

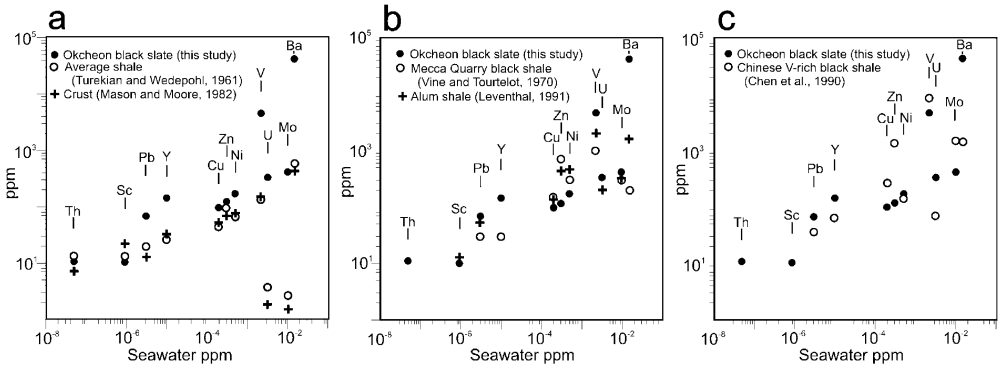

Fig. 11 Plot of metal contents in carbonaceous sedimentary rocks vs seawater. Data of the Okcheon black slate are the average of samples (this study) whose carbon contents exceed 10 wt%

rich shale of the South China Block, and the (Ba, V)-muscovite-rich black slates would be the metamorphic analogue of vanadian illitic shale of the South China Block.

Both the chemical signatures and a close association with stone coal and phosphatic nodules support the concept that the OMB black slate is probably a metamorphic analogue of the Early Cambrian vanadian black shale in the South China Block that was deposited in a dysoxic marine basin. However, it is not clear whether the two basins were closely related in their ages and were interconnected with each other. Because the original sedimentary fabrics, mineralogy, and fossils of the OMB, metasedimentary rocks have almost disappeared owing to the intense metamorphism, complex thrust faulting and folding, a biostratigraphic correlation with the Chinese black shales and radiogenic isotopic dating of the depositional ages could not be conducted. The Korean Peninsula has been long considered a part of the North China (Sino-Korean) Block, but recent studies support the idea that the Korean Peninsula resulted from the collision between the South and North China Blocks (Ree et al. 1996, 2001; Yin and Nie 1993). Most tectonic models suggest that the Kyonggi Massif and the OMB are part of the South China Block, and the Yongnam Massif and the Taebaeksan Zone are connected to the North China Block. Recent reports on the Early Permian peak metamorphism (280–290 Ma) of the OMB suggest that the OMB and the weakly metamorphosed Taebaeksan Zone were separated from each other and then amalgamated later (Cheong et al. 2003; Kim et al. 2001). The Early Permian ages of peak metamorphism of the OMB should be further interpreted with regard to the collision of the North and South China Blocks because the collision in China occurred in Triassic. However, Chang (2004) stated that the entire Korean Peninsula is a part of the Sino-Korean craton and that the OMB is an aulocogen on the plate boundary. More study is required to solve the Early Cambrian paleogeography and tectonic history of the OMB. The mineralogy, geochemistry, and microfabrics of the highly carbonaceous metalliferous black slates support the possibility that the OMB is the northeastern extension of the Early Cambrian oxygen-poor basin of the South China Block in the former continental back-arc basin setting.

Conclusions

The carbonaceous black slates in the Okcheon Metamorphic Belt of the Korean Peninsula are enriched in Ba, V, Mo, and U, and they are exploited locally for their low-quality coal. The fine matrix is dominated by either quartz–(Ba, V)–mica–graphite or Quartz-Ba-feldspar–graphite. Submillimeter quartz-rich ellipsoids, polycrystalline elongate lenses, veinlets, and larger graphite–apatite ellipsoids of several centimeters are scattered through the fine matrix, including many minerals of rare elements. The occurrence of the black slates and elemental abundances imply the accumulation of metals from seawater. However, the high Ba content of the black slates suggests hydrothermal venting of Ba-rich fluids into an organic-rich marine basin. The occurrence of barite and the low quantity of sulfides indicate rather dysoxic conditions. Although a direct temporal and spatial correlation was not possible because of the intense metamorphism and multiple deformations, the enrichment of Ba and V, their close association with the graphite-apatite nodules, and the low-quality coal suggest that the black slates in the Okcheon Metamorphic Belt are metamorphosed analogues of the Early Cambrian V–Ba deposits hosted by the black shales in the South China Block.

Acknowledgements This research was supported by the Korea Science and Engineering Foundation (Project KOSEF R01-2000-000-00053-0). Comments from A.C. Brown, R.I. Grauch, and an anonymous reviewer improved the manuscript.

References

Arthur MA, Sageman BB (1994) Marine black shales: depositional environments of ancient deposits. Annu Rev Earth Planet Sci 22:499–551

Chang KH (2004) Okchon metamorphic belt and yellow-sea transform fault. Annual Meeting of the Geological Society of Korea. pp 71–72 (Abstract)

Chen N, Yang X, Liu D, Xiao X, Fan D, Wang L (1990) Lower Cambrian black rock series and associated stratiform deposits in southern China. Chinese Journal of Geochemistry 8:244–255

Cheong C-S, Jeong GY, Kim H, Choi M-S, Lee S-H, Cho M (2003) Early Permian peak metamorphism recorded in U–Pb system of black slates from the Ogcheon metamorphic belt, South Korea, and its tectonic implication. Chem Geol 193:81–92

Cho M, Kim H (2002) Metamorphic evolution of the Ogcheon metamorphic belt: review of recent studies and remaining problems. Journal of the Petrological Society of Korea 11: 121–137

Chough SK, Kwon ST, Ree JH, Choi DK (2000) Tectonic and sedimentary evolution of the Korean peninsula: a review and new view. Earth-Sci Rev 52:175–235

Cluzel D, Cadet JP, Lapierre H (1990) Geodynamics of the Ogcheon Belt (South Korea). Tectonophysics 183:41–56

Coveney RM, Chen N (1991) Ni–Mo–PGE–Au–rich ores in Chinese black shales and speculations on possible analogues in the United States. Miner Depos 26:83–88

Coveney RM, Martin SP (1983) Molybdenum and other heavy metals of the Mecca quarry and Logan quarry shales. Econ Geol 78:132–149

Coveney RM Jr, Grauch RI, Murowchick JB (1994) The geologic setting of precious metal-bearing Ni–Mo ore beds. Soc Econ Geol Newsletter 18:1, 6–11

Douville E, Bienvenu P, Charlou JL, Donval JP, Fouquet Y, Appriou P, Gamo T (1999) Yttrium and rare earth elements in fluids from various deep-sea hydrothermal systems. Geochim Cosmochim Acta 63:627–643

Fan D (1983) Polyelements in the Lower Cambrian black shale series in southern China. In: Augustithis SS (ed) The significance of trace elements in solving petrogenetic problems and controversies. Theophrastus, Athens, pp 447–474

Holland HD (1979) Metals in black shales—a reassessment. Econ Geol 74:1676–1679

Jeong GY, Kim YH (1999) Goldmanite from the black slates of the Ogcheon belt, Korea. Mineral Mag 63:253–256

Jeong GY, Lee SH (2001) Form of molybdenum in the Carbonaceous black slates of the Ogcheon Belt. Journal of the Mineralogical Society of Korea 14:52–57

Kang J-H, Lee CG (2003) Geological structures of Okcheon Metamorphic Zone in the Goesan area, Korea. Journal of the Geological Society of Korea 39:99–114

Kim H, Cho M (1999) Polymetamorphism of Ogcheon Supergroup in the Miwon area, central Ogcheon metamorphic belt, South Korea. Geosci J 3:151–162

Kim H, Cheong C-S, Cho M, Jeong GY, Choi MS (2001) Geochronologic evidence for Late Paleozoic orogeny in the Ogcheon metamorphic belt, South Korea. In: Abstracts of the Annual Meeting of the Geological Society of America, Paper No. 157-0, Boston, MA, 5–8 Nov 2001

Kim JH (1989) Geochemistry and genesis of the Guryongsan (Ogcheon) uraniferous black slate. J Korean Inst Mining Geol 22:35–63

Koh HJ, Kim JH (1995) Deformation sequence and characteristics of the Ogcheon Supergroup in the Goesan area, central Ogcheon belt, Korea. Journal of the Geological Society of Korea 31:271–298

Kříbek B, Hladíková J, Žák K, Bendl J, Pudilová M, Uhlík Z (1996) Barite-hyalophane sulfidic ores at Rozna Massif, Czech Republic: Metamorphosed black shale-hosted submarine exhalative mineralization. Econ Geol 91:14–35

Lee D-J (1986) Mineralogy of low-grade uranium ores in the black slate of the Ogcheon Group, Korea. J Korean Inst Mining Geol 19:133–146

Lee MS, Chon HT (1980) Geochemical correlations between uranium and other components in U-bearing formations of Ogcheon Belt. J Korean Inst Mining Geol 13:241–246

Lee DS, Chang KH, Lee HY (1972) Discovery of Archaeocyatha from Hyangsanri Dolomite Formation of the Ogcheon System and its significance. Journal of the Geological Society of Korea 18:191–197

Lee DS, Yun S, Lee JH, Kim JT (1986) Lithological and structural controls and geochemistry of uranium deposits in the Ogcheon black-slate formation. J Korean Inst Mining Geol 19:19–41

Lee H-Y, Yu KM, Lee SJ (1989) Microfossils from the limestone pebbles of the Hwanggangri Formation and the Hyangsanri Dolomite in the Okcheon zone, South Korea. Journal of the Paleontological Society of Korea 5:91–101

Lee CH, Lee HK, Shin M-A (1996) Geochemistry vanadium-bearing coal formation in metapelite of the Ogcheon Supergroup from the Hoenam area, Korea. Econ Environ Geol 29:471–481

Lee K-S, Chang H-W, Park, K-H (1998) Neoproterozoic bimodal volcanism in the central Ogcheon belt, Korea: age and tectonic implication. Precambrian Res 89:47–57

Leventhal JS (1991) Comparison of organic geochemistry and metal enrichment in two black shales: Cambrian Alum Shale and Devonian Chattanooga Shale of United States. Miner Depos 26:104–112

Li YH (1991) Distribution patterns of the elements in the ocean: a synthesis. Geochim Cosmochim Acta 55:3223–3240

Long H-B, Long J-C, Zhong Y-R, Zhuang S-J, Liu T (1994) Existence of hyalophanite in the Zhangcun-Zhengfang black shales vanadium deposits: evidence for a hydrothermal genesis. Chin Sci Bull 39:1824–1827

Lott DA, Coveney RM, Jr, Murowchick JB, Grauch RI (1999) Sedimentary exhalative nickel–molybdenum ores in South China. Econ Geol 94:1051–1066

Mason B, Moore CB (1982) Principles of geochemistry. Wiley, New York

Min K, Cho M (1998) Metamorphic evolution of the northwestern Ogcheon metamorphic belt, South Korea. Lithos 43:31–51

Murowchick JB, Coveney RM Jr, Grauch RI, Eldridge CS, Shelton KL (1994) Cyclic variations of sulfur isotopes in Cambrian stratabound Ni–Mo–(PGE–Au) ores of southern China. Geochim Cosmochim Acta 58:1813–1823

Na KC, Lee DJ, Kim KH, Kim JT (1988) Study on the graphitization and stable isotope ratios of carbonaceous materials in metapelites of Ogcheon Group. Journal of the Geological Society of Korea 5:91–101

Oh CH, Kim ST, Lee JH (1995) The PT condition and timing of the main metamorphism in the southwestern part of the Okcheon metamorphic belt. Journal of the Geological Society of Korea 31:343–361

Peter JM, Simoneit BRT, Kawka OE, Scott SD (1990) Liquid hydrocarbon-bearing inclusions in modern hydrothermal chimneys and mounds from the southern trough of Guymas Basin, Gulf of California. Appl Geochem 5:51–63

Ree J-H, Cho M, Kwon S-T, Nakamura E (1996) Possible eastward extension of Chinese collision belt in South Korea: the Imjingang Belt. Geology 24:1071–1074

Ree JH, Kwon SH, Park YD, Kwon ST, Park SH (2001) Pre-tectonic and post-tectonic emplacements of the granitoids in the south central Okcheon belt, South Korea: implications for the timing of strike–slip shearing and thrusting. Tectonics 20:850–867

Shim JC, Moon H-S, Oh JH (1995) Mineralogy of graphitic nodules distributed in black shales in the Ogcheon Group. Journal of the Mineralogical Society of Korea 8:108–117

So C-S, Kang J-K (1978) Mineralogy and geochemistry of uranium-bearing black slates in the Ogcheon Group, Korea. Journal of the Geological Society of Korea 14:93–102

Steiner M, Wallis E, Erdtmann B-D, Zhao Y, Yang R (2001) Submarine-hydrothermal exhalative ore layers in black shales from South China and associated fossils—insights into a Lower Cambrian facies and bio-evolution. Palaeogeogr Palaeoclimitol Palaeoecol 169:165–191

Turekian KK, Wedepohl KH (1961) Distribution of the elements in some major units of the Earth's crust. Geol Soc Amer Bull 72:175–191

Vine JD, Tourtelot ER (1970) Geochemistry of black shale deposits—a summary report. Econ Geol 65:253–272

Yin A, Nie S (1993) An indentation model for the North and South China collision and the development of the Tan-Lu and Honam fault systems, eastern Asia. Tectonics 12:801–813